In This Issue

CellPress

Kites of the Protein World

PAGE 2183

Three distinct SMC complexes are needed for proper chromosome maintenance and segregation in eukaryotes. Palecek and Gruber reveal that Smc5/6 complexes—but not cohesin and condensin—share structurally conserved tandem WH domain subunits with their prokaryotic relatives. Potential functional and evolutionary implications are discussed.

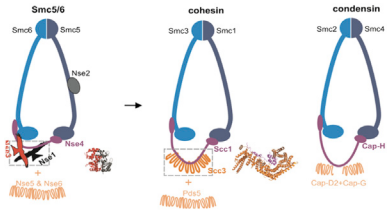

How Eukaryotic Hsp70s Work

PAGE 2191

Hsp70s play a key role in protein folding and homeostasis. Yang et al. determined structures of human Hsp70 BiP in the ATP-bound state and the isolated SBD with a peptide bound. These structures and biochemical analysis revealed the molecular mechanism of substrate binding and allosteric coupling in eukaryotic Hsp70s.

Supersizing Hemocyanin

PAGE 2204

Gai et al. determined an X-ray crystal structure of intact molluscan hemocyanin, which unveiled the architecture of the 3.8-MDa cylindrical supermolecule composed of hierarchically associated homologous functional units. Roles of the inner collar domains and carbohydrates, and evolutionary implications are discussed in detail.

How Cyclopropanation Happen

PAGE 2213

Khare et al. report crystal structures of an NADPH-dependent cyclopropanase and two enoyl reductases. The importance of a ''cyclopropanase loop'' in determining the unusual activity is shown with a chimeric enzyme.

Negative Allosteric Regulation of Pin1

PAGE 2224

Pin1 is a two-domain cell-cycle enzyme that catalyzes the *cis-trans* isomerization of phospho-S/T-P motifs. Wang et al. use NMR to examine Pin1 mutants and reveal a phosphopeptide substrate that reduces interdomain contact while enhancing isomerase activity; this suggests negative allosteric regulation of the catalytic site by interdomain contact.

Extracellular Loops Help OprG Transport Its Cargo

PAGE 2234

Kucharska et al. solved the solution NMR structures of the *P. aeruginosa* membrane protein OprG and a Pro mutant with a compromised amino acid transport function through the outer membrane of this Gram-negative pathogen.

From Transient Protein States to Mutant p53 Drugs

PAGE 2246

Joerger et al. determine structures of the p53 cancer mutant Y220C in complex with stabilizing small molecules, revealing that some of these molecules target a transiently open subpocket. These data provide a framework for the design of potent molecules for personalized anticancer therapy.

Changing Dynamics of an Active-Site Loop Changes Everything

PAGE 2256

Using NMR and computational approaches, Gagné et al. demonstrate that a single residue mutation away from the site of reaction significantly alters conformational integrity and binding properties in RNase A, demonstrating the large effects caused by small structural changes on long-range conformational dynamics and ligand specificities.

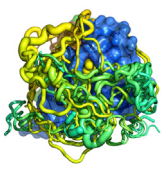

Unfuzzing the Pin1/c-Myc Fuzzy Complex

PAGE 2267

Using an integrated structural biology approach, Helander et al. provide insights into how the structural ensemble of a disordered Myc region specifically binds to the regulatory protein Pin1 to govern cell growth and differentiation.

Ligand-Binding Mechanism in Steroid Receptors

PAGE 2280

Edman et al. combine X-ray crystallography, computational simulations, and residence time measurements to uncover the ligand entry and exit processes of steroid hormone receptors. Subsequent bioinformatic analyses confirm that differences in the details of the ligand entry mechanism lead to differential selection pressure across the receptor family.

The Importance of Ligand-Receptor Conformational Pairs in GPCRs

PAGE 2291

Miller et al. identify a correlation between antagonist-induced receptor thermal stability and G protein recruitment inhibition via BRET and use this strategy to obtain two co-crystal structures of the opioid receptor NOP. Docking studies point to a mechanism for antagonist-induced receptor stabilization.

Dynamic Short Hydrogen Bonds in M2 Proton Channel

PAGE 2300

Miao et al. have characterized the full-length M2 proton channel from Influenza A by solid-state NMR in liquid crystalline lipid bilayers. Hydronium ions attack short hydrogen-bonded His37 pairs, followed by proton release, to yield either a futile or proton-conducting cycle through the charged histidine tetrad.

H95 is a pH-Dependent Gate in AQP4

PAGE 2309

Kaptan et al. demonstrate that AQP4 permeability is regulated via a conserved histidine residue, H95. The regulation is dependent on the protonation state of the residue and is sensitive to cytoplasmic pH conditions. A mutation of H95 to alanine abolishes the pH sensitivity of AQP4.

Helicase Domain of DNA Polymerase

PAGE 2319

Newman et al. describe a structure of an unusual helicase domain of DNA polymerase theta (Polθ). The helicase-like domain of Polθ forms tetramers, and this tetrameric structure might bring together broken DNA ends for microhomology-mediated end joining.

Time-Lapse Crystallography of PKA

PAGE 2331

Das et al. observe the formation of the Michaelis complex of the catalytic subunit of Protein Kinase A using time-lapsed X-ray crystallography. The structures reveal important geometric transitions in and around the active site that precede the phosphoryl transfer reaction.

Human Programmed Death-1 (PD-1) and Its Ligand PD-L1

PAGE 2341

Zak et al. reveal the molecular details of the human PD-1/PD-L1 interaction based on an X-ray structure of the complex. The authors elucidate that the ligand binding to human PD-1 is associated with significant plasticity within the receptor and provide a detailed molecular map of the interaction surface.

NAIP5/NLRC4 Inflammasome

PAGE 2349

Diebolder et al. use cryo-electron tomography and subtomogram averaging to show that flagellin-induced NAIP5/NLRC4 inflammasomes form helical polymers. Rigid body fitting of dormant NLRC4 crystal structure subdomains indicate that LRR domain rotation accompanies NLR activation. This might also be relevant for other NLR-containing inflammasomes.

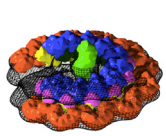

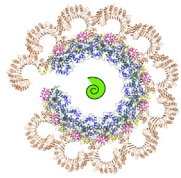

Role of a Conserved Solvent Network in Activation of Opsin

PAGE 2358

The 2.3 Å resolution crystal structure of bovine opsin stabilized in an activated conformation reveals an extensive solvent-mediated hydrogen-bonding network, linking the chromophore site to motifs important for GPCR activation and to the G protein-binding site.

In This Issue

CellPress

γ-TEMPy Gets You There

PAGE 2365

Pandurangan et al. develop a genetic algorithm to simultaneously fit multiple atomic components into low-resolution 3D-EM density maps. The method is tested on simulated and experimental benchmarks with resolutions between 10 Å and 23.5 Å. It identifies native topologies for assemblies containing up to eight components.

A New Way To Do Virtual Drug Discovery for GPCRs

PAGE 2377

Norn et al. demonstrate that a data-driven GPCR-ligand docking protocol, based on a library of mutational data, can explain the ligand structure activity relationship. In contrast to standard comparative receptor modeling, the resulting models are of practical use for virtual screening in drug discovery applications.